International Journal of Applied Research in Mechanical Engineering

Volume 2 | Issue 3 Article 9

January 2013

Design And Analysis of Rotation Rate Sensor - Modeling of vibratory MEMs Gyroscope

Priya.P. Shreshtha
Mechanical Department, Rajaram Bapu institute of Technology Islampur, Dist. Sangli, India – 415414,
shreshtha.priya@gmail.com

Sushas S. Mohite
Mechanical Department, Government College of Engg, Karad, Dist. Karad, India - 415124,
mohitess@yahoo.com

Recommended Citation

Shreshtha, Priya.P. and Mohite, Sushas S. (2013) "Design And Analysis of Rotation Rate Sensor - Modeling of vibratory MEMs Gyroscope," *International Journal of Applied Research in Mechanical Engineering*: Vol. 2: Iss. 3, Article 9.
DOI: 10.47893/IJARME.2013.1085
Available at: https://www.interscience.in/ijarme/vol2/iss3/9

DESIGN AND ANALYSIS OF ROTATION RATE SENSOR

Modeling of vibratory MEMs Gyroscope

[1]Priya.P.Shreshtha & [2]Sushas S.Mohite

[1]Mechanical Department, Rajaram Bapu institute of Technology Islampur, Dist. Sangli, India – 415414
[2]Mechanical Department, Government College of Engg, Karad, Dist. Karad, India - 415124
E-mail : shreshtha.priya@gmail.com, mohitess@yahoo.com

Abstract **-** The present work provides a detailed account of design and analysis for a typical comb-driven capacitively sensed microgyroscope. The general approach pursured in this paper is to show the possibility of achieving wide-bandwidth frequency responses in drive mode of vibratory gyroscope. Towards this goal one major design concept were discussed.

Keywords*-MEMs gyroscope,*

I. INTRODUCTION

MEMS, the acronym of "Micro-Electro-Mechanical Systems", is generally considered as devices and systems integrated with mechanical elements, sensors, actuators, and electronic circuits on a common silicon substrate through microfabrication technology. Even though an extensive variety of micromachined gyroscope designs and operation principles exists, almost all of the reported micromachined gyroscopes use vibrating mechanical elements to sense angular rate.

The concept of utilizing vibrating elements to induce and detect Coriolis force involves no rotating parts that require bearings, and have been proven to be effectively implemented and batch fabricated in different micromachining processes [5].

The vibratory gyroscope can be represented by a two degree of freedom spring-mass- damper system as shown in Figure 2. The proof-mass is driven into oscillation in the X-direction (drive mode) of the gyroscopic frame by the force *Fd*. When the proof-mass is subjected to an external rotation in the Z-direction, the induced Coriolis force causes the mass to oscillate in the Y-direction (sense mode).

The magnitude of the sense oscillation is proportional to the rotation rate of the device

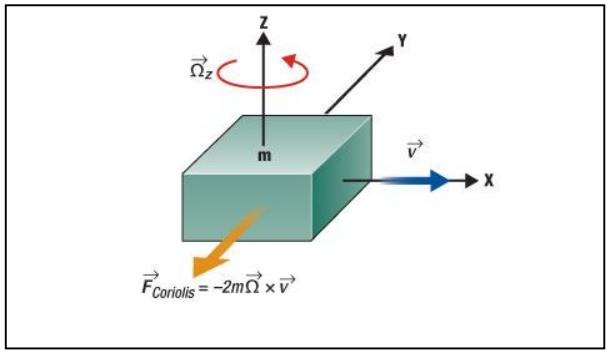

Fig. 1 : Concept of coriolis force

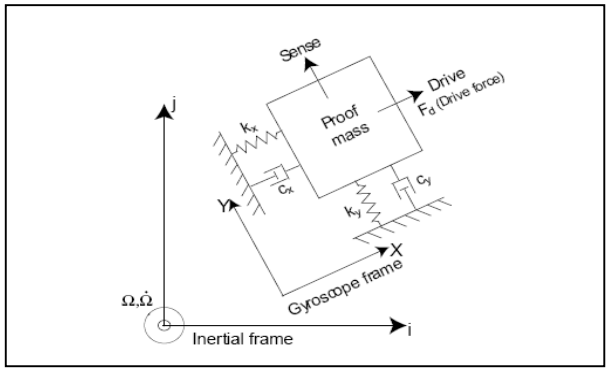

Fig. 2 : Operating principle of Vibrating Gyroscope

The 2-DOF system has two frequencies, the drive frequency $\omega_x = \sqrt{K_x/m}$ and the sense frequency $\omega_y = \sqrt{K_y/m}$ When the stiffnesses are made equal $k_x = k_y$, the sense and drive modes frequencies are matched $\omega_x = \omega_y$. Now if the system is driven with a force F_d at the

system's natural frequency, the system goes into resonance in the drive mode, maximizing drive oscillation amplitude. If the system is now subjected to a rotation about the Z-axis, the Coriolis force generated excites the sense mode in resonance, maximizing the response amplitude. For operation, the central movable mass is activated by electrostatic driving force $F_d\ (t)$ along x-direction (driving mode). Assume F_0 is a constant driving force and ω_x is the driving frequency, the electrostatic driving force is in a sinusoidal format:

$$F_d(t) = F_0 \cos \omega_x t \qquad (1)$$

Then, if the system rotates around the z-axis (normal to the paper plane) with an angular velocity of Ω, an alternating force in the y-direction is induced by Coriolis effect. Thus, the system is driven into vibration in the y-direction with a frequency of ω_y. According to the figure1, a mass m with velocity $v(t)$ along x-direction, which is in a reference frame with an angular velocity Ω along z-direction, will experience a Coriolis force $F_C(t)$ along y-direction:

$$F_C(t) = 2m\, v(t)\, \Omega \qquad (2)$$

By using some sensing schemes to measure the vibration amplitude in sensing mode, we can know the value of the angular velocity [7].

II. SIMPLE OUT-OFF PLANE SENSING MEMS GYROSCPE

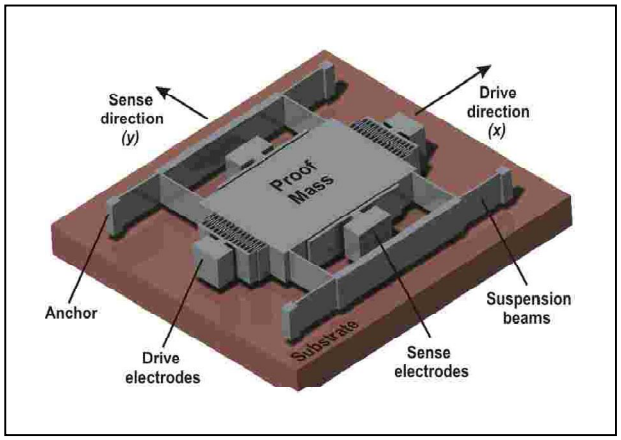

Fig. 3 : A generic MEMS conventional vibratory rate gyroscope.

Design and analysis of polysilicon and single crystal silicon gyroscopes have been carried out. Designs that utilize in-plane and out-of-plane sensing are studied. The operation principle of the vast majority of all existing micromachined vibratory gyroscopes relies on the generation of a sinusoidal Coriolis force due to the combination of vibration of a proof-mass and an orthogonal angular-rate input. The proof mass is generally suspended above the substrate by a suspension system consisting of flexible beams.

The overall dynamical system is typically a two degrees-of-freedom (2-DOF) mass-spring-damper system, where the rotation-induced Coriolis force causes energy transfer to the sense-mode proportional to the angular rate input. In most of the reported micromachined vibratory rate gyroscopes, the proof mass is driven into resonance in the drive direction by an external sinusoidal electrostatic or electromagnetic force.

$$F_{el\text{-}comb} = 4\, N\, \varepsilon_0\, (t/y)\, V_{dc} V_{ac} \qquad (3)$$

Where $\varepsilon_0 = 8.854 \times 10^{-12}$ F/m is the dielectric constant, N is the number of the fingers of the comb drive, t and y is the thickness and gap of the comb fingers and V is the applied voltage across the comb fingers. When the gyroscope is subjected to an angular rotation, a sinusoidal Coriolis force is induced in the direction orthogonal to the drive-mode oscillation at the driving frequency. Ideally, it is desired to utilize resonance in both the drive and the sense modes, to attain the maximum possible response gain, and hence sensitivity. This is typically achieved by designing and electrostatically tuning the drive and sense resonant frequencies to match. Alternatively, the sense-mode is designed to be slightly shifted from the drive-mode to improve robustness and thermal stability.

Consider a single proof mass with a structure of 500 x 500 μm^2 area which is suspended by four beams[2].

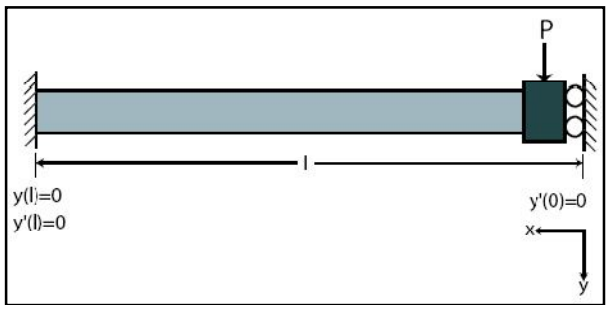

Figure : 4 Guided Beam.

The four beams have a guided beam end condition as shown in figure 4. The parameter selected for suspension are listed in table I. Since all the four beams move in parallel in both in-plane and out-of-plane directions, the stiffness of the individual beam is added to get the total structural stiffness. The expression for stiffness and the effective mass of guided beam is taken as:

$K_x = 4E\, t_b\, W_b^3 / l_b^3$ and $K_z = 4E\, W_b\, t_b^3 / l_b^3$

$M_{eff} = (13/35)m$ (4)

Material properties of Design-1 are selected for silicon with modulus of elasticity E = 169 GPa. Poisons ratio =0.22 and density of material as 2300 Kg/m^3. Area of proof mass is 500 X 500 μm^2. Using the equivalent mass we compute the natural frequency of the structure with the formula:

$$F = (1/2\pi)\sqrt{K_{eq}/m_{eq}} \quad (5)$$

The suspension design for this simple gyroscope are analyzed. This design employs the hammock suspension. The main advantage of this suspension is that it is easy to design, as there are only two design variables, the width of the beam and the length of the beam. The thickness of the structure is decided by the process. A small mismatch in the natural frequencies is introduced by fixing the width of the beam to be lesser than the thickness. Results of the simulation show that for a design 1 gives a resolution of 1.03º/s with a scale factor of 0.0001. The bandwidth i.e the sensors useful frequency range observed is 378.3 Hz

Table – I Susspension Parameters Of Design-1

Parameters	**Values**
Beam Length (l_b)	300µm
Beam width (W_b)	3.3µm
Beam Thickness (t_b)	3.5µm
In-plane stiffness (K_x) (N/m)	3.149
Out-of-plane stiffness (K_z)(N/m)	3.540

TABLE – II : TWO MODES OF FREQUENCIES OF DESIGN -1

Operating mode	**Frequency (Analytical)**	**Frequency (ANSYS)**	**Percentage Difference**
Drive mode (x-direction)	6277.18	6365	1.4
Sense mode (z-direction)	6655.48	6699.5	0.6

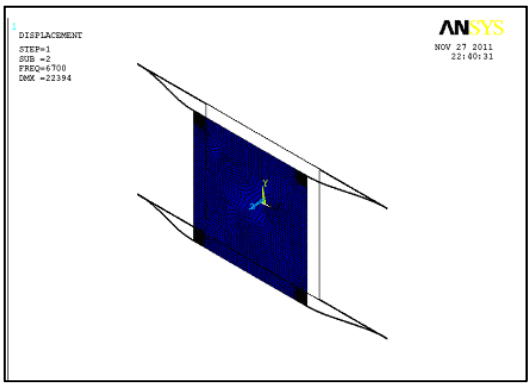

Fig 5 : Out-of-plane motion of proof-mass. (6700Hz)

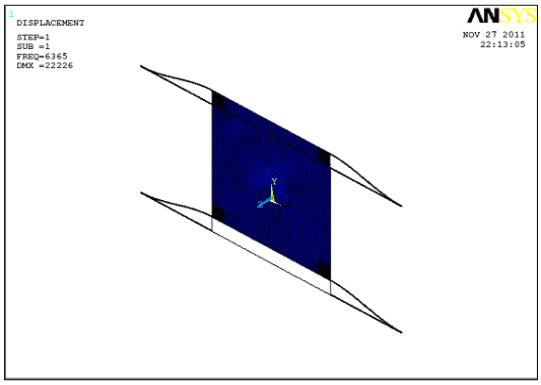

Fig. 6 In-plane motion of proof-mass. (6365 Hz).

The percentage difference is calculated by normalizing the ANSYS data with the analytical values. As seen in TableII, the values of the frequencies computed by the analytical formulas agree well with the values obtained in ANSYS. For the ANSYS analysis, the gyro structure was meshed with shell elements with the guided boundary conditions applied at the nodes connecting the flexure beams with the proof-mass. The bandwidth i.e the sensors useful frequency range observed is 378.3 Hz

III. Z-AXIS IN- PLANE SENSING MEMS GYROSCOPE

The Z-Axis gyroscope is commonly referred to as the yaw rate sensor. The yaw sensor has both the sense and drive modes in the plane of the device [3]. The structure has a symmetric suspension. In this design, the comb fingers are not directly attached to the proof-mass but are placed on the side, top and bottom plates as shown in Figure 7. These plates are connected to the proof-mass through an assembly of suspension beams. In the drive mode, the horizontal beams do not deform due to high axial stiffness. Similarly, in the sense mode the displacements of the vertical beams are negligible. This

property of the structure leads to decoupled oscillation modes as the comb fingers on the top and bottom plates only move in the presence of the Coriolis force and not during driving motion. The capacitance change due to the sense motion is picked up by comb fingers in the sense direction [1].

Consider a single proof mass with a structural of 500 x 500 μm^2 area which is suspended by eight horizontal and eight vertical beams. The parameters selected for suspension are listed in table III. Material properties of z-axis gyroscope are selected for silicon with modulus of elasticity E = 169 GPa. Poisons ratio =0.22 and density of material as 2300 Kg/m^3.

Table – III : Susspension Parameters Of Z-axis Gyroscope

Parameters	**Values**
Beam Length (l_b)	75µm
Beam width (W_b)	2µm
Beam Thickness (t_b)	2µm
In-plane stiffness (K_x) (N/m)	51.27
Out-of-plane stiffness (K_z)(N/m)	51.27

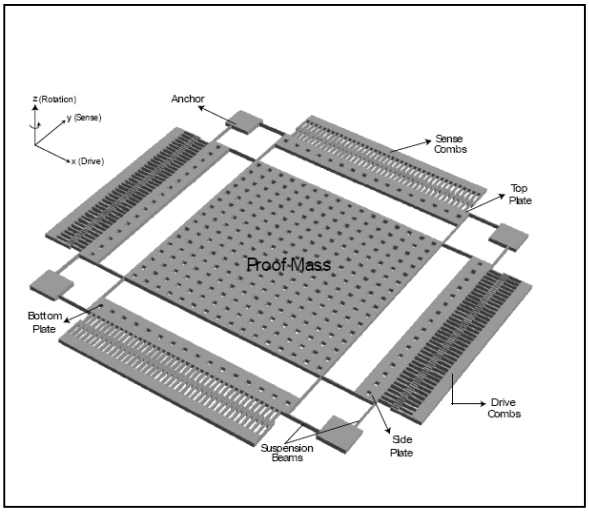

Fig. 7 : Z-axis gyroscope.

Area of proof mass is 500 X 500 μm^2. The stiffness in the drive direction is the sum of the stiffnesses of the eight vertical beams under flexure. Similarly, the stiffness in the sense direction is the sum of the stiffnesses of the eight horizontal beams [3]. All the beams have equal cross-sections and lengths. This leads to the stiffness in the drive and sense directions to match. The expressions for the stiffness in the drive and sense modes is given by

$$K_x = K_y = (8E\, t_b w_b^3) / l_b^3 \qquad (6)$$

TABLE IV : Two Mode Frequencies Of Z-axis Gyroscope

Operating mode	**Frequency (Analytical)**	**Frequency (ANSYS)**	**Percentage Difference**
Drive mode (x-direction)	28363	29583	4.3
Sense mode (y-direction)	28363	29583	4.3

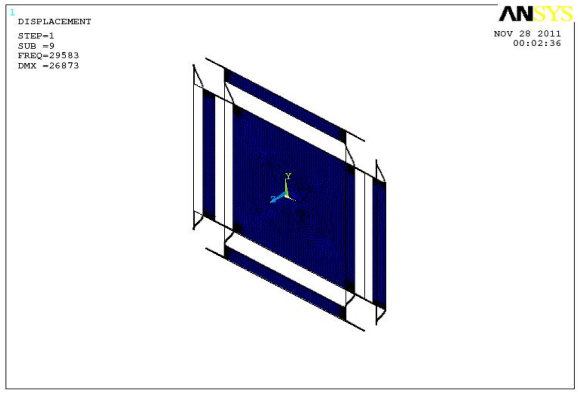

Fig. 8 : motion in drive mode(x-direction).

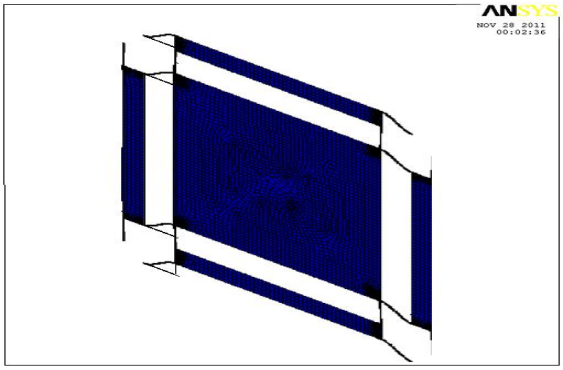

Fig. 9 : motion in sense mode (y-direction).

IV. TUNING FORK GYROSCOPE

The tuning fork gyroscope is a very popular concept for a vibrating-element angular rate sensor. It works on the principle of balanced induced coriolis forces. In order to compensate for linear velocities and accelerations, two symmetric vibrating elements are used in a tuning-fork configuration [7]. The vibrating element called tines, are vibrated in phase towards each other. With the application of a rotation rate, a secondary lateral vibration is induced in both tines, as shown in figure10

The suspension employs folded beam flexures. The advantage of folded beams is that they relieve residual stresses that develop in the structural layer during

fabrication. The folded beams are anchored near the proof-mass as shown in Figure11. This allows the expansion and contraction of the four beams connected to the proof-mass along the x-axis, allowing relief of built-in residual stress[10]. Residual stresses causes buckling in the structure, which leads to reduction in performance. Although this structure is relatively insensitive to built-up residual stress, the suspension is more complicated [4].

Consider two proof masses with a structure of 500 x 500 μm^2 area which are suspended by total eight folded beams. Material properties of tuning fork gyroscope are selected for silicon with modulus of elasticity E = 169 GPa. Poisons ratio =0.22 and density of material as 2300 Kg/m^3.

$$Ky = Ky_1 + Ky_2 + Ky_3 + Ky_4 \quad (7)$$

$$Kz = Kz_1 + Kz_2 + Kz_3 + Kz_4 \quad (8)$$

$$Ky_1 = (E\, t_{b1} w_{b1}^3) / l_{b1}^3 \quad (9)$$

$$Kz_1 = (E\, w_{b1} t_{b1}^3) / l_{b1}^3 \quad (10)$$

Similar for beam 2, 3 and 4 as shown in figure 11. The parameters selected for suspension are listed in table V.

TABLE – V : Susspension Parameters Of Tuning Fork Gyroscope

Parameters	**Values**	**Parameters**	**Values**
Beam Length (l_{b1})	300µm	Beam width(W_{b1})	2.8µm
Beam Length (l_{b2})	100µm	Beam width(W_{b2})	4.2µm
Beam Length (l_{b3})	500µm	Beam width(W_{b3})	50µm
Beam Length (l_{b4})	200 µm	Beam width(W_{b4})	15 µm

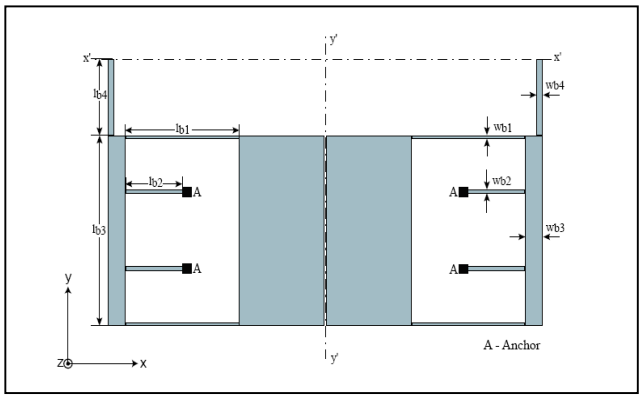

Fig. 10 : Structural Parameters of Tuning Fork

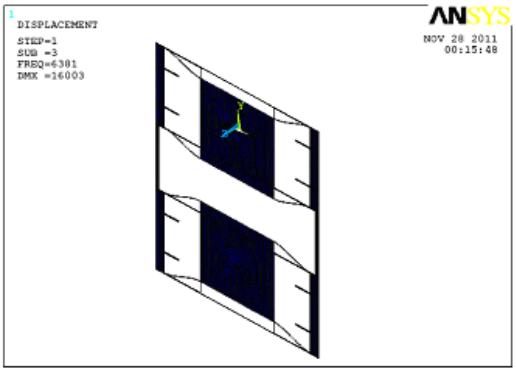

Figure 11 : Tuning Fork Gyroscope.

Figure : 12 In and out motion of masses at frequency 6381Hz.

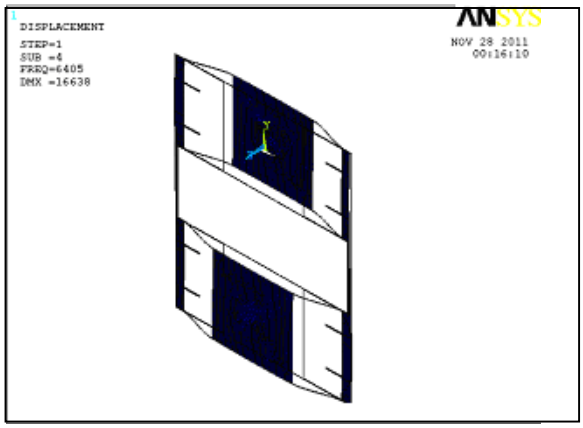

Figure 1. In and out motion of masses at frequency 6405 Hz.

TABLE : IV : TWO MODE FREQUENCIES OF TUNING FORK GYROSCOPE

Operating mode	**Frequency (Analytical)**	**Frequency (ANSYS)**	**Percentage Difference**
Drive mode (x-direction)	28363	29583	4.3
Sense mode (y-direction)	28363	29583	4.3

V. ENHANCEMENT OF BAND-WIDTH BY INCREASING DEGREES OF FREEDOM.

The 3-DOF design aims to utilize resonance in either drive-mode or sense-mode to improve the sensitivity while maintaining the robust operational characteristics. Figure 15 illustrates the 3-DOF design concept. In the 3-DOF system with 2-DOF drive-mode, the wide band region is achieved in the drive-mode frequency response. By utilizing the dynamic amplification in the drive-mode, large oscillation amplitude of the sense element is achieved with the

small actuation amplitudes providing improved linearity and stability even with parallel plate actuation.

A. 3-DOF System with 2-DOF Drive-Mode.

Such types of Gyroscopes are operated at resonance in the sense-mode to achieve maximum sense-mode amplitudes and the wide bandwidth frequency region is achieved in the drive-mode. The overall 3-DOF Micromachined Vibratory Gyroscopes consist of two interconnected proof masses *m1* and *m2* as shown in Figure 14. Mass *m1* is excited in the drive direction (x-axis) whereas it is constrained not to oscillate in sense direction. For the driving purpose of the gyroscope, a standard comb drive actuation mechanism is being used. This is very well proven mechanism to obtain large linear displacements. However large drive voltages are required and the resultant force of comb drive is low. Mass *m2* can oscillate both in drive and sense direction (y-axis). In this way the gyroscope dynamical system consists of a 2-DOF drive-mode oscillator along with 1-DOF sense-mode oscillator. Mass *m2*, thus forms the passive mass of the 2-DOF drive-mode oscillator and acts as the vibration absorber of mass *m1*.

In the sense direction *m2* defines a resonant 1-DOF oscillator. When an external angular rate is applied about the z-axis, the Coriolis force is induced on *m2* and only *m2* responds to this Coriolis force. This response of the sense-mode is detected by the parallel plate sensing electrode. Since the dynamical system is 1-DOF resonator in the sense direction, the frequency response of the device has a single resonance peak in the sense-mode. For the purpose of defining the operational frequency region of the system sense direction resonance frequency should lie within the flat region of the 2-DOF drive oscillator. This allows the operation at resonance in sense direction for improved sensitivity, while the drive direction amplitude is inherently constant in the same frequency band, in spite of parameter variations [7].

Almost all existing Micromachined Vibratory Gyroscopes operate on the principle of detection of rotation induced Coriolis force in the presence of an angular rate input. So the proof mass should be free to oscillate in two orthogonal directions, and desired to be constrained in other vibration modes. Therefore suspension system design plays an important and critical role in achieving these objectives. Figure 15 illustrates the folded flexures attached with the drive as well as sense mass. The suspension that connects the mass m_1 with the substrate via anchors is comprised of four, double-folded flexures. Eeach beam of length L_{1x} in the folded flexure can be modeled as a fixed-guided beam.

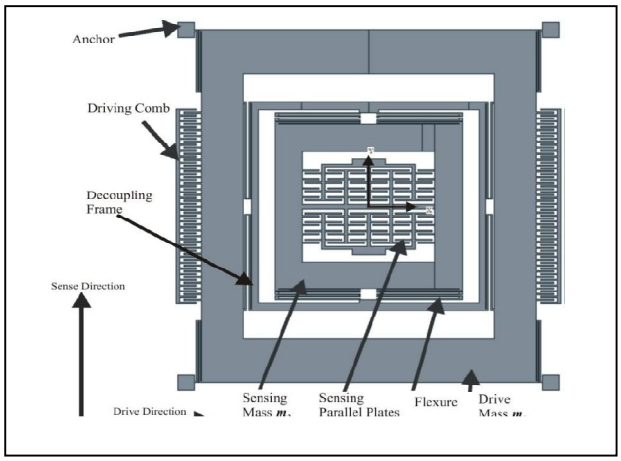

Figure 14 : Micromachined Vibratory Gyroscopes with 2-DOF drive-mode.

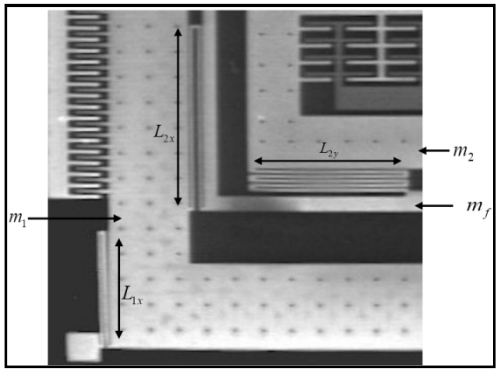

Fig. 15 : The folded flexures attached with the drive and sense mass.

deforming in the orthogonal direction to the axis of the

$$k_1 x = \frac{4}{2}\left(\frac{1}{2}\frac{3EI}{\left(\frac{L_{1x}}{2}\right)^3}\right) = \frac{2Etw^3}{{L_{1x}}^3} \qquad (11)$$

beam, leading to an overall stiffness of [2]

where E is the Young"s Modulus, I=tw^3/12 is the second moment of inertia of the beam cross section, 't' is the beam thickness and 'w' is the beam width. Decoupling frame having mass m_f is connected to m_1 via four double-folded flexure,(each beam with length of L_{2x}) that can be deformed in the drive direction resulting in the drive direction stiffness values of

$$k_2 x = \frac{4}{2}\left(\frac{1}{2}\frac{3EI}{\left(\frac{L_{2x}}{2}\right)^3}\right) = \frac{2Etw^3}{L_{2x}^{\ 3}} \qquad (12)$$

Sensing mass m_2 is connected to decoupling frame with four five-folded flexures each having beam length of L_{2y}. Since these flexures are stiff in drive direction and deform only in sense direction, instability due to dynamical coupling between drive and sense-mode in the sensing element m_2 is eliminating. So the overall stiffness with the length of L_{2y} for each beam is

$$k_{2y} = \frac{4}{5}\left(\frac{1}{2}\frac{3EI}{\left(\frac{L_{2y}}{2}\right)^3}\right) = \frac{4Etw^3}{5L_{2y}^{\ 3}} \qquad (13)$$

B. Analytical Evaluation.

A 3-DOF gyroscope is designed for demonstration of design concept having following dynamical system parameters:

The proof mass values are m1=2.208 X 10^{-9}Kg, m2=1.15 X 10^{-9}Kg and decoupling frame mass mf= 7.65 X 10^{-10} Kg. The spring constants are K_{1x} = 0.656 N/m, K_{2x} =0.126 N/m and K_{2y} =0.2N/m. Thus for the drive mode-oscillation the active and passive proof mass values become m_{1x}=2.208 X10^{-9}Kg, m_{2x} =1.915 X 10^{-9} Kg. IN drive mode the resonant frequencies of the isolated active and passive mass-spring systems are $\omega_{1x} = \sqrt{K_{1x}/m_{1=}}$ 7243 Hz and $\omega_{2x} = \sqrt{K_{2x}/(m_f + m_2)}$ = 1290 Hz respectively. Yielding a frequency ratio of $\gamma_x = \omega_{2x}/\omega_{1x}$ =0.47 and a mass ratio of $\mu_x = (m_2+m_f)/m_1$ = 0.8673. With this parameters the location of the two expected resonance peaks were calculated as $F_{x\text{-}n1}$= 1161.58 Hz and $F_{x\text{-}n2}$ = 3048.17 Hz based on relations as follows.

$$\omega_{x-n1} = \sqrt{\frac{1}{2}\left(1+\mu_x+\frac{1}{\gamma_x^2}-\sqrt{\left(1+\mu_x+\frac{1}{\gamma_x^2}\right)^2-\frac{4}{\gamma_x^2}}\right)}\omega_{2x} \qquad (14)$$

$$\omega_{x-n2} = \sqrt{\frac{1}{2}\left(1+\mu_x+\frac{1}{\gamma_x^2}+\sqrt{\left(1+\mu_x+\frac{1}{\gamma_x^2}\right)^2-\frac{4}{\gamma_x^2}}\right)}\omega_{2x} \qquad (15)$$

TABLE-VII : Drive And Sense Frequencies of 3-DOF Model

Operating mode	Frequency (Analytical)	Frequency (ANSYS)	Percentage Difference
Drive mode (m1)	1161.58	917.055	0.3
Drive mode (m2 + mf)	1290	1095	0.2
Sense mode (m2)	2098.87	1724.00	0.2

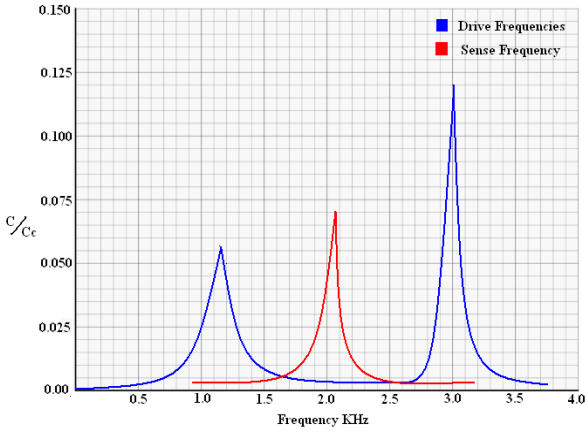

Fig. 16 : Structural Parameters of Tuning Fork

VI. CONLUSION.

The bandwidth i.e the sensors useful frequency range observed is 378.3 Hz and that for three degree of freedom design it is 1887.54 Hz. The major advantage of the 3-DOF system with 2-DOF drive-mode is the ability to achieve large drive-mode oscillation amplitudes in the drive-mode passive-mass, while the oscillation amplitudes of the driven masses are drastically suppressed. This allows utilizing parallel-plate actuators with small gaps to produce large drive-mode amplitudes with low actuation voltages. The damping factor (C/ C_C) decreases as we reduce the gap between proof mass and substrate. In design 1 Perforations are generally provided on the proof-mass to enable the release of the structure. They also perform the additional function of reducing squeeze film damping effects in the out-of-plane modes.

ACKNOWLEDGMENT

I thanks to Dr. Mohite. S. S. for introducing me the amazing culture and philosophy behind MEMS. I also greatly appreciate the life-long support of my dear parents and continuous encouragement of my dear husband.

REFERENCES

[1] Sensing of the time-varying angular rate for MEMS Z-axis gyroscopes M.H. Salah a, M.L. McIntyre b, D.M. Dawson c, J.R. Wagner d, E. Tatlicioglu e,*

[2] Modeling and performance study of a beam microgyroscope M. Ghommema, _, A.H.Nayfeh a, S.Choura b, F.Najar b, E.M.Abdel-Rahman c

[3] Design, modelling and simulation of a High Frequency MEMS Gyroscope in 1.5um SOI P.J.Nganaa,c*, J.J.Koningc, P.J. Frencha, J.J.M Bontempsb,c, K. Seetharamanb,c

[4] Detection capacitance analysis method for tuning fork micromachined gyroscope based on elastic body model Tao Jiang a,∗, Anlin Wang b, Jiwei Jiao c, Guangjun Liu a

[5] Design and simulation of an angular-rate vibrating microgyroscope S. Rajendrana,K.M,Liewa,b,∗

[6] An Approach for Increasing Drive-Mode Bandwidth of MEMS Vibratory Gyroscopes Cenk Acar and Andrei M. Shkel, *Associate Member, IEEE, Associate Member, ASME.*

[7] Two Types of Micromachined Vibratory Gyroscopes Andrei M. Shkel Mechanical & Aerospace Engineering University of California Irvine Irvine, CA, USA ,Cenk Acar BEI Systron Donner Automotive Division Concord, CA, USA, Chris Painter BAE Systems Inertial Products Westlake Village, CA, USA

[8] A parametrically amplified MEMS rate gyroscope Z.X. Hua, B.J. Gallachera,∗, J.S. Burdessa, C.P. Fell b, K. Townsendb

[9] Structural design and analysis of micromachined ring-type vibrating sensor of both yaw rate and linear acceleration. Jui-Hong Wenga, Wei-Hua Chienga, Jenn-Min Laib

[10] A multiple-beam tuning-fork gyroscope with high quality factors Ren Wanga, Peng Chenga, Fei Xiea, Darrin Youngb, Zhili Haoa

◈◈◈